



Research paper

Position Tracking Control of ASV based on Dynamic Inversion with Intelligent Methods

Heydar Toossian Shandiz * Mohsen Erfani Haji Pour and Amir Ali Bagheri

Faculty of Engineering, Ferdowsi University of Mashhad, Mashhad, Iran.

Article Info

Article History:

Received 21 January 2024

Revised 19 June 2024

Accepted 22 August 2024

DOI:10.22044/jadm.2024.14081.2516

Keywords:

Dynamic inversion control, fuzzy methods, Perceptron neural network, Ship dynamics, Position Tracking

*Corresponding author:
htoossian@um.ac.ir (H. Toossian Shandiz).

Abstract

This article discusses the development of an efficient controller for precise tracking of Autonomous Surface Vehicles (ASVs) using dynamic inversion control techniques. ASVs face challenges from environmental disturbances such as waves and winds, which are crucial for industries like maritime transport and military operations requiring high navigation accuracy. This article proposes an approach that integrates classical control with intelligent methods to mitigate disturbances and correct modeling errors. Two distinct dynamic inversion controller-based methods are proposed: one utilizes a perceptron neural network with an adaptive term to compensate for modeling errors in the dynamic inversion controller, and the other employs fuzzy logic to adjust control parameters for modeling error reduction. The aim of these methods is to enhance system flexibility and path-tracking accuracy. Evaluation criteria include step response analysis and the ability to track complex paths, with comparisons against the conventional PID control method showing favorable results.

1. Introduction

Dynamic positioning (DP) systems are a cornerstone of the modern marine industry, critical for the precise navigation and station-keeping of various vessels such as drilling ships, warships, and research vessels. The significance of DP systems lies in their ability to enhance operational efficiency, safety, and environmental protection. By automatically maintaining a ship's position and path, DP systems enable complex marine operations that would be otherwise infeasible, such as deep-sea drilling, subsea construction, and emergency response in adverse weather conditions. DP systems leverage computer-controlled algorithms to manipulate a vessel's propellers and thrusters, maintaining its desired position by counteracting external forces like wind, waves, and currents. These systems rely on a network of sensors, including

position sensors, motion sensors, gyroscopes, and wind sensors, to gather critical data. The onboard computer processes this data to calculate the necessary propulsion power and steering angles, ensuring the vessel remains on its intended course [1,2]. DP systems were first used for offshore drilling during the 1960s. As drilling moved into deeper waters, portable rigs were no longer feasible, and anchoring in deep water was uneconomical. In 1961, the first vessel equipped with four rotating thrusters used a dynamic positioning system to retrieve nuclear samples from the Earth's second layer. Later, these systems were developed for other purposes, such as tracking on target tracks [3]. However, the dynamic and often harsh marine environment presents significant challenges for maintaining precise control. Environmental disturbances, such as fluctuating winds, waves,

and ocean currents, introduce nonlinearities and uncertainties that control methods struggle to handle effectively. This has spurred extensive research into advanced nonlinear control theories over the past few decades, aiming to improve the robustness and accuracy of DP systems under varying conditions.

Up until now, several control systems have been developed for ship control purposes. One of the classical control methods is the PID control method, which has been utilized to design a system that guarantees asymptotic stability for ships. The proposed controller has a simple and intuitive structure [4-6]. The H_∞ control method has also been employed to design a system that ensures asymptotic stability and acceptable tracking performance subject to disturbances [7,8]. In addition, a robust adaptive control method has been designed by integrating the observer and the Backstepping method, resulting in a robust adaptive control law [9]. Another control method involves an adaptive sliding mode control algorithm with output feedback and an adaptive mechanism for estimating the upper bound of unknown disturbances. Based on the simulation outcomes, it is evident that the control technique suggested in this research demonstrates resilience when confronted with different obstacles such as uncertainties in the model, noise in measurements, limitations in inputs, and disturbances [10]. The control system for the ship is mathematically represented through a model, and the control challenge is formulated utilizing the framework of a Markov decision process. Reinforcement learning is then utilized to teach an optimal control method for the ship system, which is more accurate and flexible than traditional control methods. This control method can also be customized for different working and environmental conditions [11]. Another proposed method suggests an approach using a Takagi-Sugeno (T-S) fuzzy model with stochastic actuator failures. By considering sampling intervals, a suitable Lyapunov-Krasovskii function (LKF) is constructed to achieve mean square exponential criteria to ensure optimal tracking performance [12]. Another control method proposes a fast terminal sliding mode control

approach with adaptive settings for dynamically positioned (DP) ships. This method aims to enhance the positioning accuracy and anti-interference performance of ships against uncertain dynamic model parameters and varying environmental disturbances. The stability and convergence of the system are proven using the adaptive law and Lyapunov stability criteria [13]. Another proposed method introduces the use of second-order differential equations and invariant control theory. The presented model considers the ship as a dynamic object in a six-dimensional coordinate system. This approach provides high accuracy in ship position control by taking into account all measurable state vector coordinates, speed, and displacement [14]. In addition to the mentioned methods, a new nonlinear model predictive control (NMPC) algorithm for dynamic positioning of ships, using the Laguerre function to describe control increment signals, can be referenced. This method significantly reduces the computation compared to traditional MPC algorithms while maintaining the control performance. This approach effectively addresses challenges arising from the nonlinear nature of ship movement, input saturation, and environmental disturbances, ensuring rapid and precise real-time ship positioning [15]. Finally, an improved sample data control method for dynamically positioned ships using the Takagi-Sugeno fuzzy model can be mentioned. By introducing second-order time conditions and a reciprocal convex approach, the new Lyapunov-Krasovskii function (LKF) fully utilizes sampling information and reduces conservatism. Stability conditions, robust performance, state uncertainty, and controller design are analyzed using linear matrix inequalities (LMIs) [16].

The objective of this article is to develop a robust control mechanism for autonomous ships that effectively tracks desired paths using the dynamic inversion (DI) controller. Unlike conventional nonlinear control methods that often rely on linearized system equations and linear feedback approaches, the DI method employs feedback linearization to directly handle the inherent nonlinearities of the system

dynamics. This approach facilitates the approximation of complex dynamic equations, which are inherently nonlinear, into more manageable linear forms. A key focus of this study is to mitigate environmental disturbances and address modeling inaccuracies. To achieve this, the article proposes the integration of neural network (NN) and fuzzy methods within the control framework. These intelligent techniques are utilized to adaptively tune control parameters and enhance the system's robustness against external disturbances. In the context of autonomous ship control, the proposed DI-based control systems are rigorously evaluated and compared against the traditional PID control method. This comparative analysis aims to underscore the superior performance of the DI-based approaches in terms of both disturbance rejection and path-tracking accuracy. In essence, this research aims to contribute to advancing the state-of-the-art in autonomous ship navigation by leveraging advanced nonlinear control methodologies. By addressing the challenges posed by environmental disturbances and modeling complexities, the proposed DI-based control systems demonstrate their potential to significantly enhance the operational reliability and performance of autonomous marine vessels.

The article is organized as follows:

Section 2 presents the equations that govern the ship's behavior, while Section 3 describes the proposed approach, which involves designing a DI control system and incorporating intelligent methods. Section 4 discusses the results of the simulation and analysis, and Section 5 presents the conclusion of the study.

2. Dynamic model of the ship

Generally, a ship has six degrees of freedom of movement. However, when designing control systems for ships, not every degree of freedom is taken into account.

The selection of which degree of freedom to use in a particular model depends on the purpose of the controller and the ship's existing actuators. The analysis is centered on the ship's movement in the horizontal plane, with a particular emphasis on examining three degrees of freedom. This examination takes into account the ship's motion and dynamics in terms of its position, velocity, and

orientation in the horizontal plane. By considering this case, a complete understanding of the ship's behavior and its response to external forces and disturbances is possible [17].

The movement of the ship on the surface of the water can be described by the coordinate systems of the inertial dimension and the fixed-body dimension.

The ship's state variables for movement are represented by two vectors, namely $\hat{v} = [u, v, r]^T$ and $\eta = [x, y, \psi]^T$. The ship's position is represented by the coordinates x and y , while its heading is denoted by ψ , u and v are the components of the linear velocities in the direction of surge and sway and r is the yaw rate [17-19].

The velocity vector determined in the inertial frame is connected to the velocity vector determined in the body-fixed frame through the following kinematic relationship:

$$\dot{\eta} = R(\psi)\hat{v} \quad (1)$$

$$R(\psi) = \begin{bmatrix} \cos(\psi) & -\sin(\psi) & 0 \\ \sin(\psi) & \cos(\psi) & 0 \\ 0 & 0 & 1 \end{bmatrix} \quad (2)$$

Where $R(\psi)$ is the rotation matrix by angle ψ .

According to equations 1 and 2, we will have:

$$\dot{x} = u\cos(\psi) - v\sin(\psi) \quad (3)$$

$$\dot{y} = u\sin(\psi) + v\cos(\psi) \quad (4)$$

$$\dot{\psi} = r \quad (5)$$

The dynamic model of the ship can be expressed as follows: [3, 17-19]:

$$M\dot{\hat{v}} + C(v)\hat{v} + D(v)\hat{v} = \tau + R^T(\psi)b = \tau + \tau_d \quad (6)$$

The inertia matrix as the following relation:

$$M = \begin{bmatrix} m - X_{\dot{u}} & 0 & 0 \\ 0 & m - Y_{\dot{v}} & mX_G - Y_r \\ 0 & mX_G - N_v & I_z - N_r \end{bmatrix} \quad (7)$$

Where m is the mass, $X_{\dot{u}}$, $Y_{\dot{v}}$ and etc. are hydrodynamic derivatives and I_z is the moment of inertia about the fixed z -axis of the ship.

The Coriolis matrix is also defined as the following relationship:

$$C = \begin{bmatrix} 0 & 0 & -m_{22}v - m_{23}r \\ 0 & 0 & m_{11}u \\ m_{22}v + m_{23}r & m_{11}u & 0 \end{bmatrix} \quad (8)$$

The positive damping matrix defined as the following equation:

$$D = \begin{bmatrix} -X_u & 0 & 0 \\ 0 & -Y_v & -Y_r \\ 0 & -N_v & -N_r \end{bmatrix} \quad (9)$$

The control vector input is made up of surge force, sway force, and yaw torque, and is expressed as the following equation:

$$\tau = [\tau_x, \tau_y, \tau_n]^T \quad (10)$$

The unmodeled external low-frequency forces and moments will be a constant bias as follows:

$$b(t) = [b_1(t), b_2(t), b_3(t)]^T \quad (11)$$

The external disturbances that are applied to the ship in the fixed reference frame of the body are defined as the following relationship:

$$\tau_d = R^T(\psi)b = \begin{bmatrix} b_1 \cos(\psi) + b_2 \sin(\psi) \\ -b_1 \sin(\psi) + b_2 \cos(\psi) \\ b_3(t) \end{bmatrix} \quad (12)$$

The resulting velocity vector for the ship is expressed as the following relationship [17-19]:

$$V = \sqrt{u^2 + v^2} \quad (13)$$

3. Control system design

In this section, the designed control system is discussed.

3.1. Dynamic inversion control system

The DI control system is one of the nonlinear control methods based on feedback linearization. In this approach, the nonlinear system is converted into a linear system, after this conversion, the system can be controlled with well-known and practical methods of linear control [20, 21].

The dynamics of the nonlinear system are considered as the following relationship:

$$\dot{x} = f(x, u) \quad (14)$$

$$y = Cx$$

In order to establish a direct relationship between the input and output, the derivative of the output is taken until the input variable appears in the equation.

$$y^{(r)} = F(x) + G(x)u \quad (15)$$

Now using the pseudo-control v we will have:

$$u = \frac{1}{G(x)}(v - F(x)) \quad (16)$$

$$y^{(r)} = v \quad (17)$$

To compensate for the error and get the output to the reference, we have:

$$v = Ke \quad (18)$$

$$e = y_d - y \quad (19)$$

Where K is a linear controller.

According to equations (3) to (5), it can be seen that the input did not appear in the first derivative of the

output, so to reach the desired relationship, the derivative is taken from these relationships:

$$\ddot{x} = \dot{u} \cos(\psi) - \dot{\psi} u \sin(\psi) - \dot{\psi} v \cos(\psi) - \dot{v} \sin(\psi) \quad (20)$$

$$\ddot{y} = \dot{u} \sin(\psi) + \dot{\psi} u \cos(\psi) - \dot{\psi} v \sin(\psi) + \dot{v} \cos(\psi) \quad (21)$$

$$\ddot{\psi} = \dot{r} \quad (22)$$

The second derivative of the output can be written as a combination of linear and nonlinear expressions:

$$\begin{bmatrix} \ddot{x} \\ \ddot{y} \\ \ddot{\psi} \end{bmatrix} = \begin{bmatrix} F_x \\ F_y \\ F_\psi \end{bmatrix} + G \begin{bmatrix} \tau_x \\ \tau_y \\ \tau_n \end{bmatrix} \quad (23)$$

Based on equation (18), we will have:

$$\begin{bmatrix} \ddot{x} \\ \ddot{y} \\ \ddot{\psi} \end{bmatrix} = \begin{bmatrix} v_x \\ v_y \\ v_\psi \end{bmatrix} = \begin{bmatrix} K_x(x_d - x) \\ K_y(y_d - y) \\ K_\psi(\psi_d - \psi) \end{bmatrix} \quad (24)$$

3.2. Integration of dynamic inversion control and intelligent methods

Consider the ship control system as follows:

$$\dot{x} = f(x, u) \quad (25)$$

According to the definition of pseudo-control, we have:

$$v = \hat{f}(x, u) \quad (26)$$

$\hat{f}(x, u)$ is an approximate model of $f(x, u)$. As a result, we have:

$$f(x, u) = \hat{f}(x, u) + \Delta(x, u) \quad (27)$$

$$\Delta(x, u) = f(x, u) - \hat{f}(x, u) \quad (28)$$

$\Delta(x, u)$ is the modeling error.

According to equation (25), we will have:

$$\dot{x} = v + \Delta(x, u) \quad (29)$$

To fix the modeling error and also to remove environmental disturbances, the integration of DI control method and intelligent methods can be used.

In this article, methods based on perceptron neural network (PNN) and fuzzy methods are used to solve this problem.

3.2.1. Perceptron neural network with one hidden layer

The pseudo control vector to compensate the modeling error can be considered as follows:

$$v = \ddot{x}_d + v_c - v_{NN} \quad (30)$$

In equation (30), v_c is the output of a linear controller system, which is considered here as a proportional derivative controller, v_{NN} is the adaptive term to remove the modeling error $\Delta(x, u)$ [22-30].

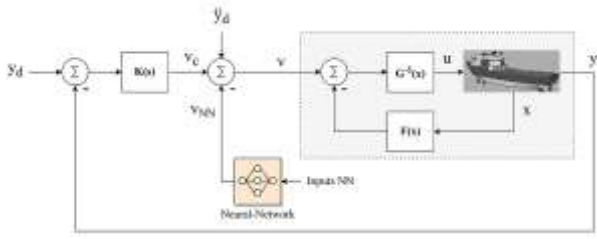


Figure 1. Control system of ship based on DI and NN method.

3.2.1.1. PNN Structure

The structure of PNN with one hidden layer can be expressed as follows:

$$y = \theta_W^k + \sum_{j=1}^{n_2} w_j^k \beta_j \quad k = 1, \dots, n_3 \quad (31)$$

$$\beta_j = \sigma(\theta_V^j + \sum_{i=1}^{n_1} v_i^j x_i)$$

In this context, n_1 , n_2 and n_3 represent the number of neurons in the input, hidden, and output layers, respectively. Also, σ is the activation function, v_i^j is the input weights, w_j^k is the output weights, θ is the bias expression.

The activation function in the network is as follows:

$$\sigma(z) = \frac{1}{1 + e^{-az}} \quad (32)$$

The β vector is also as follows:

$$\beta(z) = [1 \ \sigma(z_1) \ \dots \ \sigma(z_n)]^T \quad (33)$$

The input of PNN is considered as follows:

$$X = [1, x_d - x, x_d, \dot{x}_d, \hat{v}_{NN}, \|\dot{z}\|]^T \quad (34)$$

The Z matrix is obtained based on the input and output weights in the form of the following relationship:

$$Z = \begin{bmatrix} V & 0 \\ 0 & W \end{bmatrix} \quad (35)$$

The output of NN will be as follows:

$$v_{NN} = \hat{W}^T \beta(\hat{V}^T X) \quad (36)$$

3.2.1.2. PNN weights update law

The weight update rule of PNN is expressed as follows:

$$\dot{\hat{W}} = -\Gamma_W [(\hat{\sigma} - \hat{\sigma}' \hat{V}^T X) E^T P b + \lambda \|E\| \hat{W}] \quad (37)$$

$$\dot{\hat{V}} = -\Gamma_V [X E^T P b W^T \hat{\sigma}' + \lambda \|E\| \hat{V}] \quad (38)$$

In the defined relations, Γ_W and Γ_V are learning rates, which are positive defined, $\hat{\sigma}'$ is the partial derivative of the activation function, and λ is the error correction parameter, which are positive defined. P is positive definite and for any positive definite diagonal matrix Q is obtained based on the

Lyapunov equation $A^T P + P A = -Q$. P according to the error dynamics, that is $\dot{E} = A E + b(v_{NN} - \Delta)$ so that $E = [e \ \dot{e}]^T$ and $b = [0 \ 1]^T$, in the form of the relation (41) is considered.

$$\hat{\sigma}' = \frac{d\sigma}{dz} \Big|_{z=\hat{V}^T X} = \begin{bmatrix} 0 & \dots & 0 \\ \frac{d\sigma(z_1)}{dz_1} & \dots & 0 \\ \vdots & \ddots & \vdots \\ 0 & \dots & \frac{d\sigma(z_{n_2})}{dz_{n_2}} \end{bmatrix} \quad (39)$$

$$A = \begin{bmatrix} 0 & 1 \\ -K_p & -K_d \end{bmatrix} \quad (40)$$

Matrix A is Hurwitz. By appropriately selecting the control parameters (PD controller) K_p and K_d , the system matrix A can be made Hurwitz. Hence, this assumption is typically satisfied.

Remark 1. The point that should be noted is that it can be shown by using the Lyapunov stability theorem that the NN weights and the system error are bounded and the correct selection of Γ_W , Γ_V and λ can affect the system's control performance and robust [22-30].

$$P = \begin{bmatrix} K_d + \frac{1}{2K_p} & \frac{1}{2K_p} \\ \frac{1}{2K_p} & \frac{1 + K_d}{2K_p K_d} \end{bmatrix} \quad (41)$$

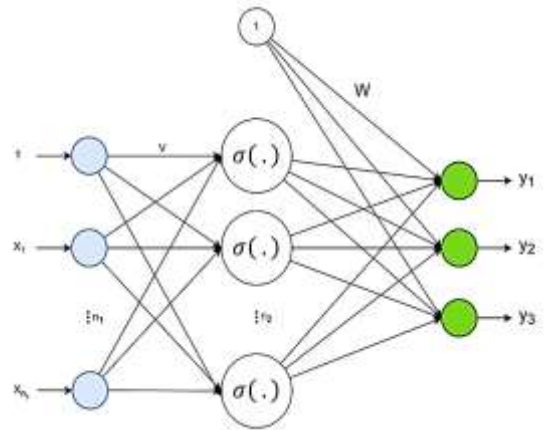


Figure 2. Perceptron neural network Structure.

3.2.2. Adjusting the gains of the linear controller by the fuzzy method

To improve performance, reduce system error, and compensate for modeling errors, a potential approach is to combine the DI control method with fuzzy logic methods. This method involves considering the linear controller $K(s)$ as a PID

controller, with control coefficients determined by applying fuzzy rules and methods.

3.2.2.1. PID controller

The PID Controller as a transfer function has the following form:

$$K_c(s) = K_p \left(1 + \frac{1}{T_i s} + T_d s \right) \quad (42)$$

The elements proportional, integral, and derivative are represented by the coefficients K_p , K_i , and K_d , respectively.

Moreover, the time constants associated with the integral and derivative components are represented by $T_i = K_p / K_i$ and $T_d = K_d / K_p$ respectively.

The discrete-time formulation of the PID controller can be expressed as follows:

$$u_k = K_p e_k + K_i T_s \sum_{i=1}^n e_i + \frac{K_d}{T_s} \Delta e_k \quad (43)$$

In this research, the control signal at time step k is symbolized by u_k while the discrepancy between the reference value and the output is denoted as e_k . The controller's sampling period is represented by T_s . Furthermore, the difference between e_k and e_{k-1} is defined as Δe_k

3.2.2.2. Fuzzy Gain Scheduling

In this context, the methodology employed involves the utilization of fuzzy reasoning and rules to generate the parameters for the controller. The values of K_p and K_d lie within the range of $[K_p^{\min}, K_p^{\max}]$ and $[K_d^{\min}, K_d^{\max}]$ respectively.

Subsequently, these parameters are normalized in the following manner:

$$K'_p = (K_p - K_p^{\min}) / (K_p^{\max} - K_p^{\min}) \quad (44)$$

$$K'_d = (K_d - K_d^{\min}) / (K_d^{\max} - K_d^{\min})$$

The determination of the PID parameters is based on e_k and Δe_k . The connection between T_i and T_d is expressed as follow:

$$T_i = \alpha T_d \quad (45)$$

Therefore, the integral gain is as follows:

$$K_i = K_p / \alpha T_d = K_p^2 / \alpha K_d \quad (46)$$

Where K'_p, K'_d and α are determined based on fuzzy rules.

Fuzzy rule: if e_k is A_i and Δe_k is B_i , then K'_p is C_i , K'_d is D_i and $\alpha = \alpha_i$. Her A_i, B_i, C_i and D_i are set fuzzy and α_i is constant and $i = 1, 2, \dots, m$.

The membership functions (MF) of fuzzy sets for the variables e_k and Δe_k are depicted in Figure 4. Figure 5 displays the MFs for fuzzy sets C_i and D_i , which can have values of either Big or Small. The

degree to which an element belongs to a specific fuzzy set is represented by the membership grade as μ , and its relation to the variable $x (= K'_p \text{ or } K'_d)$ is expressed as follows.

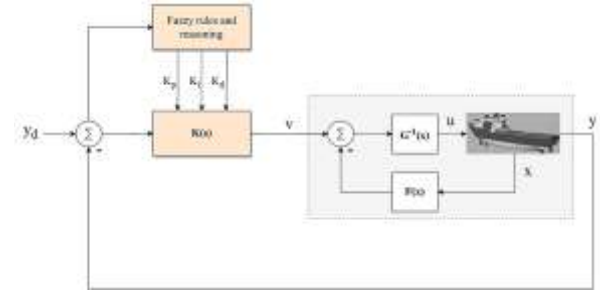


Figure 3. control system of ship based on DI method and fuzzy PID

$$\mu_x(s) = -0.25 \ln x \text{ or } x_x(\mu) = \exp(-4\mu) \quad (47)$$

for Small,

$$\mu_x(s) = -0.25 \ln(1-x) \text{ or } x_x(\mu) = 1 - \exp(-4\mu) \quad (48)$$

for Big.

If Figure 6 is a hypothetical answer. near a_1 , a lot of control signal is needed to reach the reference signal. For this purpose, the controller needs a large K_p and K_i and small K_d .

Therefore, K'_d is determined by fuzzy set small and K'_p by fuzzy set big.

When the PID controller, the integration action is increased with the inclusion of a reduced integral time constant. This can be observed as an effect of the controller's behavior. The strength of this integration process is determined by the Ziegler-Nichols adjustment law, which stipulates that the integral time constant should be four times greater than the derivative time constant. Consequently, if the integral time constant has a value of less than four, it will result in a strong integral. When the integral time constant is approximately equal to this value, the corresponding fuzzy rules are as follows. if e_k is PB and Δe_k is ZO, then K'_p is Big, K'_d is Small and $\alpha = 2$.

It should be noted that the numerical value can also be viewed as a fuzzy number, which is represented by a MF that consists of a singletone, as shown in Figure 7. For example, if α is Small, then α equals 2. To avoid excessive overshoot in the region around point a_2 as shown in Figure 6, it is recommended to use a small control signal.

In order to accomplish this objective, it is necessary for the PID controller to possess a proportional gain that is relatively small, a derivative gain that is comparatively large, and an integral gain that is relatively small. Hence, the ensuing fuzzy rule is employed:

if e_k is ZO and Δe_k is NB, then K'_p is Small, K'_d is Big and $\alpha = 5$.

Table 1 contains a set of rules that can be utilized to adjust the proportional gain. Similarly, tuning guidelines for K'_d and α are provided in Table 1. In this table, B denotes Big and S represents Small.

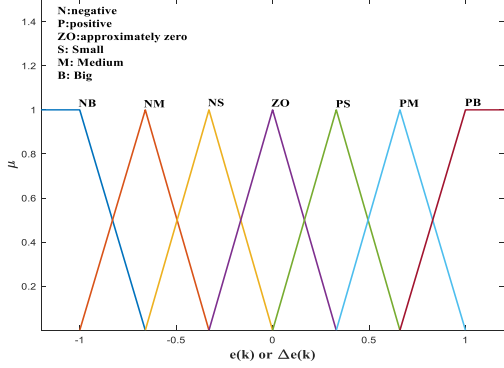


Figure 4. MFs for e_k and Δe_k .

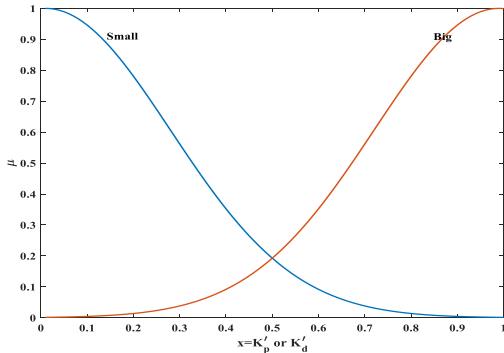


Figure 5. MFs for K'_p and K'_d .

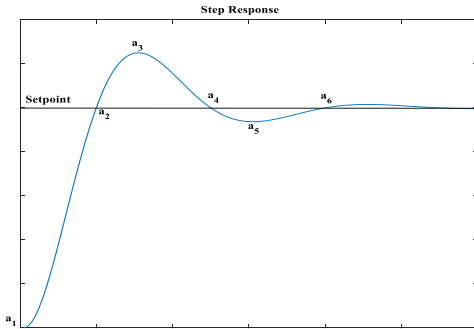


Figure 6. Step response.

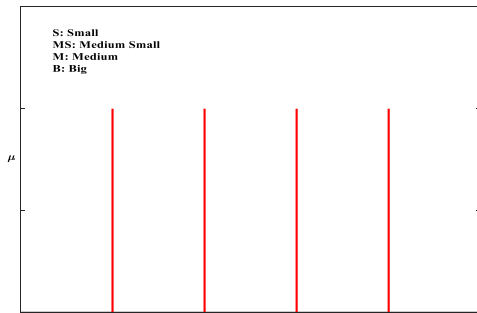


Figure 7. Singleton MFs form.

The truth value μ_i is obtained by the product of the MF values in the antecedent part of the rule:

$$\mu_i = \mu_{A_i}[e_k] \cdot \mu_{B_i}[\Delta e_k] \quad (49)$$

Where μ_{A_i} signifies the MF value of the fuzzy set A_i for a specific value of e_k , and μ_{B_i} denotes the MF value of the fuzzy set B_i for a particular value of Δe_k . The truth degree, μ_i , is employed to ascertain the values of K'_p and K'_d for each rule based on their respective MF. The implication process of a fuzzy rule is illustrated in Figure 8. By employing the MFs depicted in Figure 4, we can establish the subsequent condition:

$$\sum_{i=1}^m \mu_i = 1 \quad (50)$$

The result of the defuzzification is as follows:

$$K'_p = \sum_{i=1}^m \mu_i K_p^i \quad (51)$$

$$K'_d = \sum_{i=1}^m \mu_i K_d^i \quad (52)$$

$$\alpha = \sum_{i=1}^m \mu_i \alpha_i \quad (53)$$

The equivalence between K'_p and μ_i , expressed as a grade for the i th rule, is denoted by the variable K_p^i .

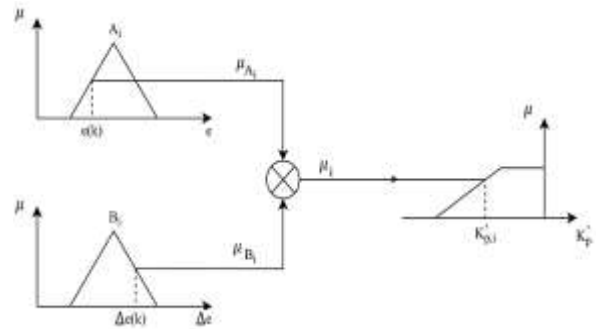


Figure 8. Implication process of a fuzzy rule.

The equations given below are utilized to determine the PID controller's parameters:

$$K_p = (K_p^{\max} - K_p^{\min})K'_p + K_p^{\min} \quad (54)$$

$$K_d = (K_d^{\max} - K_d^{\min})K'_d + K_d^{\min} \quad (55)$$

$$K_i = K_p^2 / \alpha K_d \quad (56)$$

The range of K_p and K_d has been developed based on a simulation analysis of different processes.

$$K_p^{\min} = 0.32K_u, K_p^{\max} = 0.6K_u \quad (57)$$

$$K_d^{\min} = 0.08K_u T_u, K_d^{\max} = 0.18K_u T_u$$

By [34], The gain and period of oscillation at the stability limit under proportional control are represented by the variables K_u and T_u , respectively.

Remark 2. It should be noted that the PID controller's parameters utilized in the dynamic inversion method, as discussed in this particular context, exhibit time variation. This characteristic poses a challenge in analyzing the stability closed loop system. Although asymptotic stability may be ensured, the initial transients may prove to be unsatisfactory in numerous applications. Therefore, it is desirable to have a hierarchical entity, such as a supervisor, to monitor the control system's performance.

Table 1. Fuzzy Tuning Rules.

		Δe_k						
		NB	NM	NS	ZO	PS	PM	PB
K'_p	NB	B	B	B	B	B	B	B
	NM	S	B	B	B	B	B	S
	NS	S	S	B	B	B	S	S
	ZO	S	S	S	B	S	S	S
	PS	S	S	B	B	B	S	S
	PM	S	B	B	B	B	B	S
	PB	B	B	B	B	B	B	B
K'_d	NB	S	S	S	S	S	S	S
	NM	B	B	S	S	S	B	B
	NS	B	B	B	S	B	B	B
	ZO	B	B	B	B	B	B	B
	PS	B	B	B	S	B	B	B
	PM	B	B	S	S	S	B	B
	PB	S	S	S	S	S	S	S
α	NB	2	2	2	2	2	2	2
	NM	3	3	2	2	2	3	3
	NS	4	3	3	2	3	3	4
	ZO	5	4	3	3	3	4	5
	PS	4	3	3	2	3	3	4
	PM	3	3	2	2	2	3	3
	PB	2	2	2	2	2	2	2

The supervisor can detect instability in the early stages, if present, and take appropriate corrective action. If instability is detected, the controller parameters can be adjusted to a predefined set of stabilizing parameters to ensure the stability of the control system. Alternatively, if deemed necessary, the system can be deactivated by setting the parameter to zero [32-39].

4. Simulation and Results

Simulation tests have been performed for the designed control systems and their performance has been compared with the classic PID control system.

4.1. Ship Model

The ship selected to examine and analyze the designed control system is a model ship called *CyberShip I*, which is used to determine and test the control system.

The ship under investigation is built at a scale of 1:70, having a mass of 17.6 kg and a length of 1.19 meters. By employing system identification techniques and hydrodynamic methods, the model parameters of the ship were established [3, 31].

The resulting inertia matrix is presented as follows:

$$M = \begin{bmatrix} 26.4247 & 0 & 0 \\ 0 & 51.3671 & -0.7372 \\ 0 & -0.7372 & 1.2645 \end{bmatrix} \quad (58)$$

The damping matrix is as follows:

$$D = \begin{bmatrix} 4.3411 & 0 & 0 \\ 0 & 6.2983 & 0 \\ 0 & 0 & 1.2577 \end{bmatrix} \quad (59)$$

The ship is impacted by forces and torques that are both random and vary over time.

These disturbances are considered in the following manner:

$$b_1(t) = 12 + 15 \sin(0.35t) + 5 \sin(0.25t) + 3 \sin(0.45t) \quad N \quad (60)$$

$$b_2(t) = 10 + 5 \sin(0.5t) \quad N \quad (61)$$

$$b_3(t) = 0.5 + 0.5 \sin(0.1t) \cos(0.3t) \quad Nm \quad (62)$$

4.2. Parameters of Control Systems

The PNN method has yielded the controller's parameters, which are listed below:

$$K_p = [K_p^x, K_p^y, K_p^w] = [10.3, 8.2, 53.3]$$

$$K_d = [K_d^x, K_d^y, K_d^w] = [0.93, 1.3, 2.98]$$

$$\Gamma_w = [\Gamma_w^x, \Gamma_w^y, \Gamma_w^w] = [2.2, 1.1, 1.6]$$

$$\lambda_w = [\lambda_w^x, \lambda_w^y, \lambda_w^w] = [6, 1, 0.1]$$

$$\Gamma_v = [\Gamma_v^x, \Gamma_v^y, \Gamma_v^w] = [1.1, 1.4, 1.5]$$

$$\lambda_v = [\lambda_v^x, \lambda_v^y, \lambda_v^w] = [11.1, 9.3, 11.2]$$

In addition, in the activation function in the neural network defined in relation (32), $a = 10$ is considered. In the proposed fuzzy method, the values of K_u and T_u were experimentally determined by gradually increasing the

proportional gain and observing the response of the system. When the system begins to exhibit oscillations, the proportional gain at that point is the limit of stability.

The values of these parameters are as follows:

$$K_u = [K_u^x, K_u^y, K_u^\psi] = [20, 23, 26] \quad (59)$$

$$T_u = [T_u^x, T_u^y, T_u^\psi] = [1.25, 1.5, 1.25]$$

The initial conditions are also $\eta = [0 \text{ m}, 0 \text{ m}, 0^\circ]$ and $v = [0 \text{ m/s}, 0 \text{ m/s}, 0^\circ/\text{s}]$.

4.3. Step response test

To assess the capability of the proposed methods in tracking a predefined setpoint, a step response test is conducted initially. Figure 9 illustrates the step response for each channel, while Table 2 presents performance indicators.

The outcomes demonstrate that the employment of the DI controller in combination with the fuzzy method leads to a noteworthy reduction in maximum overshoot, rise time, and settling time, highlighting the effectiveness of this approach. In the following, a more detailed analysis will be done in this direction.

1. Maximum Overshoot:

The maximum overshoot is an essential parameter indicating the extent to which the system exceeds the desired response. For the y-channel, the overshoot reduces from 91.9 % with the PID controller to 30.3% with the DI and fuzzy method. This reduction indicates improved stability and less aggressive overshooting, which is crucial for avoiding excessive stress on the system components.

2. Rise Time:

The rise time, which is the time taken for the response to rise from 10% to 90% of its final value, shows a substantial improvement. For instance, in the y-channel, the rise time decreases from 0.41 seconds (PID) to 0.19 seconds (DI with fuzzy method). This faster response time ensures quicker adaptation to changes, making the control system more responsive and efficient in dynamic environments.

3. Settling Time:

Settling time, the duration required for the system to remain within a certain range of the final value, is markedly reduced. For the ψ -channel, it drops from 6.47 seconds (PID) to 2.28 seconds (DI with fuzzy method). This rapid settling time enhances the overall performance, ensuring that the system stabilizes swiftly after disturbances.

4. Performance Index and IAE:

The IAE (Integral of Absolute Error) index further corroborates the superior performance of the DI controller combined with the fuzzy method. Figure 10 and the IAE error index demonstrate that this system has a superior performance index, showcasing lower cumulative errors over time, which translates to higher precision and accuracy in maintaining the desired position.

In addition to comparing the intelligent method DI with fuzzy method with the classic PID method, the performance of two proposed intelligent methods (DI with fuzzy method and DI with neural network) can also be compared with each other. The results show that both intelligent methods have a very favorable performance while being superior to the traditional PID method. Nevertheless, it can be seen that DI with fuzzy method is superior in most of the proposed criteria. These results show that the mentioned system can perform better by using fuzzy algorithms.

Table 2. Performance indexes of the step response.

Perform index	DI with Fuzzy method	DI with neural network	PID
Maximum overshoot(%)	x : 61.4%	x : 77.2%	x : 91.9%
	y : 30.3%	y : 30.7%	y : 100%
	ψ : 14.43%	ψ : 14.88%	ψ : 86.7%
Rise time /s	x : 0.25	x : 0.32	x : 0.37
	y : 0.19	y : 0.31	y : 0.41
Settling time (5%) /s	ψ : 0.22	ψ : 0.15	ψ : 0.27
	x : 5.17	x : 8.95	x : 12.57
	y : 2.71	y : 7.71	y : 7.16
IAE Index	ψ : 2.28	ψ : 2.17	ψ : 6.47
	x : 1.23	x : 2.02	x : 3.12
	y : 0.44	y : 0.91	y : 0.98
	ψ : 0.242	ψ : 0.21	ψ : 0.61

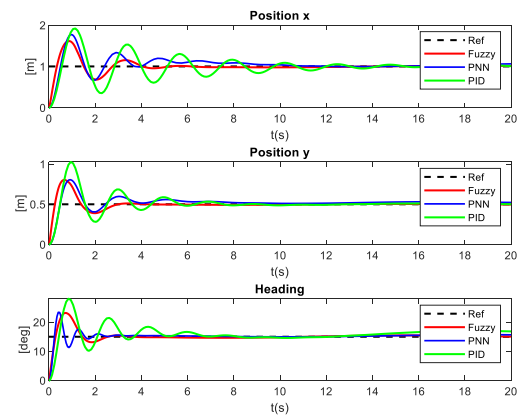


Figure 9. Step response.

Figure 12 shows the applied control forces. According to the results, in the beginning, more control force needs to be created and this force decreases as the target is approached. This high initial force ensures fast movement towards the target.

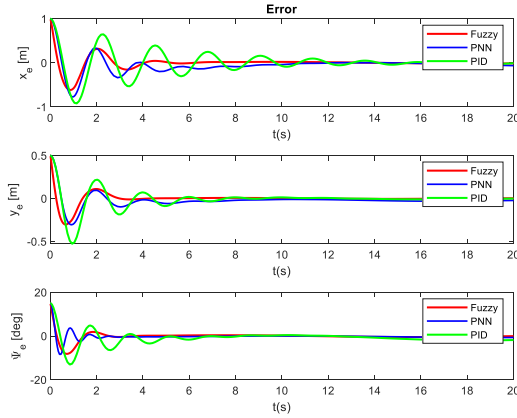


Figure 10. System error of the step response.

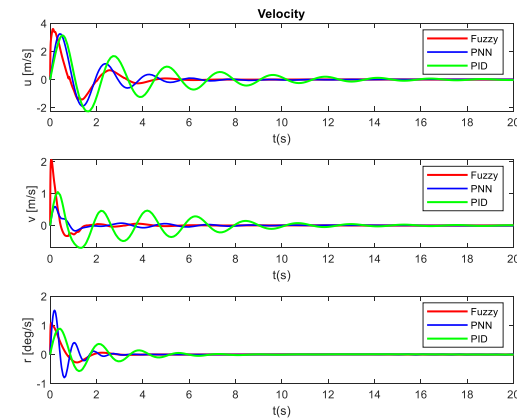


Figure 11. Velocities in control system of the step response.

Figure 13 displays the PID controller parameters used in the DI control method and the fuzzy method. The step response test clearly shows that the DI controller with intelligent methods outperforms traditional PID controllers and provides faster, more accurate, and stable responses with reduced overshoot and Settling Time. Finally, by comparing two prominent and powerful intelligent methods, fuzzy and Neural network, we can conclude the relative superiority of the fuzzy method.

4.4. Position Tracking test

This section examines the effectiveness and performance of the proposed systems in tracking a pre-established path or position. Figures 14 and 15 show the reference position tracking using the proposed methods. The results demonstrate that the combination of the DI control system and fuzzy method performs better in following the reference path with less tracking error.

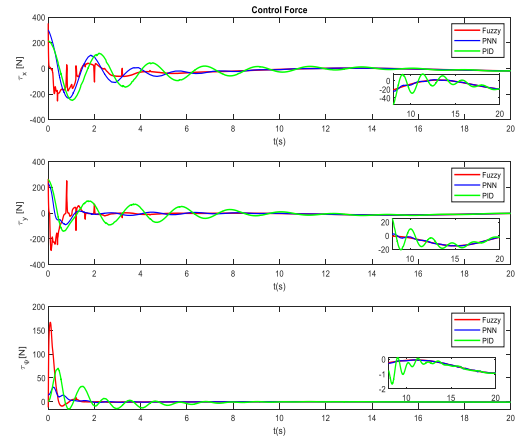


Figure 12. Control force of the step response

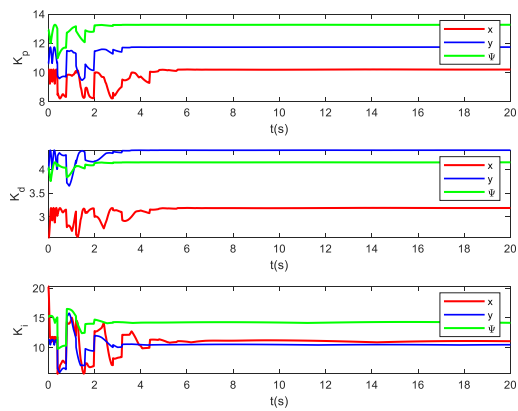


Figure 13. Tuning PID parameters for step response

The following provides a more detailed analysis:

1. Tracking Accuracy: Figures 14 and 15 show that the DI controller with the fuzzy method has higher tracking accuracy compared to traditional methods. The system follows the reference path with minimal deviation, indicating a strong and precise control mechanism.
2. Control Force: As seen in Figure 18, the control force is initially higher and gradually decreases over time. This behavior ensures that the system quickly reaches the desired path and then maintains it with minimal force, optimizing energy consumption and reducing actuator wear.
3. System Error and Speeds: Figures 16 and 17 display the system error and speeds during position tracking. The reduced error and smooth speed profiles indicate a stable and efficient control system. The

adaptability of the fuzzy method allows it to cope well with environmental disturbances and dynamic changes, maintaining a steady path.

Figures 14 to 18 also show that the DI controller with a perceptron neural network outperforms the traditional PID method and demonstrates less error in reference path tracking compared to classical methods. The neural network's learning and adaptation capabilities enhance the system's accuracy, reducing errors. The neural network's ability to learn patterns and environmental conditions gives it a superior tracking accuracy over traditional methods. Comparing the intelligent methods presented, the results indicate that the DI controller with the fuzzy method performs better than the perceptron neural network.

The fuzzy method, due to its higher adaptability and precision, has a greater ability to maintain the reference path and reduce errors.

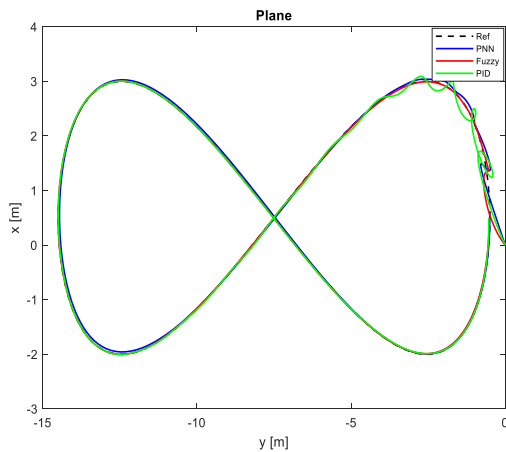


Figure 14. Position tracking in the x and y plane

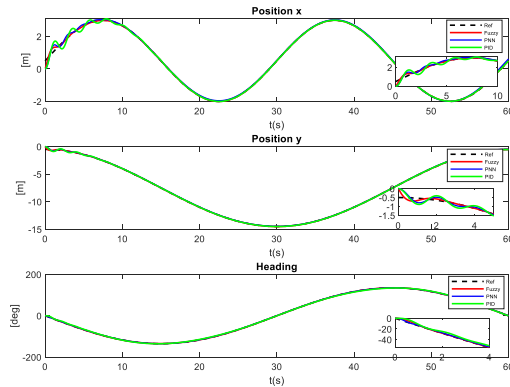


Figure 15. Tracking the position and heading of the target

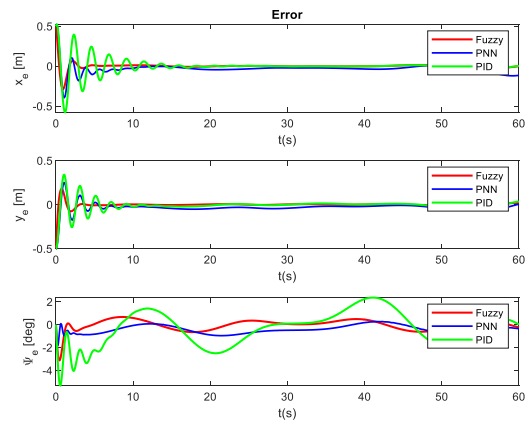


Figure 16. System error in position tracking.

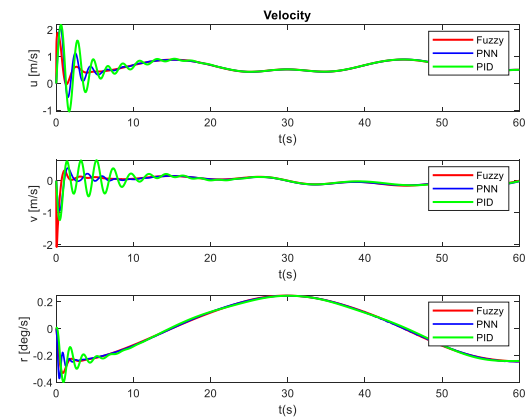


Figure 17. Velocities in the control system in position tracking.

Compared to the neural network, the fuzzy method manages control forces more optimally, particularly in channel x. As shown in Figure 18, the control force in the fuzzy method is more effectively regulated, resulting in lower energy consumption and less wear on the actuators.

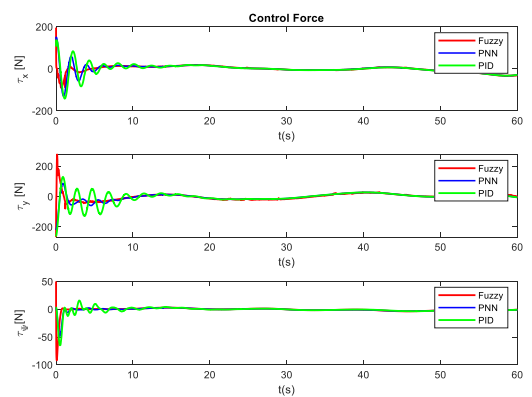


Figure 18. Control force in position tracking.

The position tracking experiment confirms that the proposed DI control system, along with the fuzzy and neural network methods, provides superior performance in tracking desired paths. While both fuzzy and neural network methods offer high accuracy, the fuzzy method, with its adaptability to different conditions, provides

greater precision and more efficient control force management.

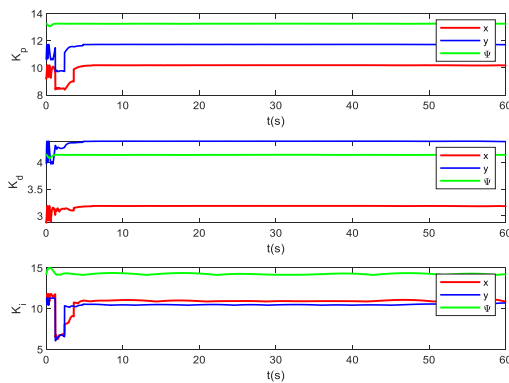


Figure 19. Tuning PID parameters in position tracking.

5. Conclusions

In this article, control systems based on the DI control method and intelligent methods were developed to achieve automatic position tracking. Neural network and fuzzy methods were employed to enhance system performance, reduce errors, and ensure robustness against environmental disturbances. The results obtained from comparing the performance of the designed control systems with the classic PID control system are as follows:

1. Adjusting the gains of the linear controller used in the DI controller through fuzzy methods leads to a significant improvement in performance indicators compared to the DI controller with neural networks and classical methods.
2. Fuzzy techniques exhibit superior flexibility towards the variations in the environment, allowing for automatic adaptation of the coefficients of the linear controller in response to changes in environmental disturbances. This leads to a considerable enhancement in the precision of horizontal position tracking.
3. Using fuzzy methods to tune the gains of the linear controller employed in the DI controller results in the highly desirable performance of the system in tracking complex trajectories.
4. The DI control method with perceptron neural network, also has a relatively good performance, and it can be said that this control method also performs better compared to classical methods.

Overall, the developed control systems based on the DI control method and intelligent techniques have shown promising results, with fuzzy methods particularly excelling in enhancing performance and adaptability. The combination of these approaches has the potential to significantly

improve automatic position tracking in various applications.

Based on the results obtained from the experiments and the analyses conducted, several future research directions and potential improvements for the proposed methods are notable, which are outlined below:

1. Improving system accuracy and stability using artificial intelligence techniques:
 - Deep Neural Networks: Utilizing deep neural networks can lead to improved accuracy and stability of the control system. These networks can enhance system performance under varying and nonlinear conditions by analyzing large and complex datasets.
 - Reinforcement Learning: Integrating reinforcement learning techniques with current controllers can enable the system to use past experiences to enhance performance and adapt to new conditions.
2. Integrating adaptive and intelligent methods to reduce errors:
 - Model Predictive Control (MPC): Implementing model predictive control, which has the ability to predict and correct system behavior, can help improve the stability and accuracy of control systems.

References

- [1] M. Fu, L. Wang, and L. Yu, "A Finite-Time Output Feedback Control Scheme for Dynamic Positioning System of Ships," *IEEE Access*, vol. 7, pp. 100638-100648, 2019
- [2] A. Veksler, T. A. Johansen, F. Borrelli, and B. Realfsen, "Dynamic Positioning With Model Predictive Control," *IEEE Transactions on Control Systems Technology*, vol. 24, no. 4, pp. 1340-1353, 2016
- [3] M. Tomera and K. Podgórski, "Control of Dynamic Positioning System with Disturbance Observer for Autonomous Marine Surface Vessels," *Sensors*, vol. 21, no. 20, p. 6723, 2021.
- [4] A. T. Humod and N. M. Ameen, "Robust nonlinear PD controller for ship steering autopilot system based on particle swarm optimization technique," *IAES International Journal of Artificial Intelligence*, vol. 2252, no. 8938, p. 8938, 2020.
- [5] R. S. Soman, F. Gopmandal, and A. Ghosh, "MIMO PID compensation for dynamic positioning of a ship," in *2018 Indian Control Conference (ICC)*, 4-6 Jan. 2018, pp. 137-142 .
- [6] Y. Su, C. Zheng, and P. Mercorelli, "Nonlinear PD Fault-Tolerant Control for Dynamic Positioning of Ships With Actuator Constraints," *IEEE/ASME*

- Transactions on Mechatronics*, vol. 22, no. 3, pp. 1132-1142, 2017.
- [7] M. Zheng, Y. Zhou, S. Yang, and L. Li, "Robust H_{∞} control of neutral system for sampled-data dynamic positioning ships," *IMA Journal of Mathematical Control and Information*, vol. 36, no. 4, pp. 1325-1345, 2019.
- [8] S. Yang and M. Zheng, "H-infinity fault-tolerant control for dynamic positioning ships based on sampled-data," *Journal of Control Engineering and Applied Informatics*, vol. 20, no. 4, pp. 32-39, 2018.
- [9] X. Hu, J. Du, and Y. Sun, "Robust Adaptive Control for Dynamic Positioning of Ships," *IEEE Journal of Oceanic Engineering*, vol. 42, no. 4, pp. 826-835, 2017.
- [10] K. Liang, X. Lin, Y. Chen, J. Li, and F. Ding, "Adaptive sliding mode output feedback control for dynamic positioning ships with input saturation," *Ocean Engineering*, vol. 206, p. 107245, 2020.
- [11] Z. Yin, W. He, C. Yang, and C. Sun, "Control Design of a Marine Vessel System Using Reinforcement Learning," *Neurocomputing*, vol. 311, pp. 353-362, 2018.
- [12] M. Zheng, Y. Su, S. Yang, and L. Li, "Reliable Fuzzy Dynamic Positioning Tracking Controller for Unmanned Surface Vehicles Based on Aperiodic Measurement Information," *International Journal of Fuzzy Systems*, vol. 25, no. 1, pp. 358-368, 2023.
- [13] H. Chen, J. Li, N. Gao, J. Han, N. Ait-Ahmed, and M. Benbouzid, "Adaptive backstepping fast terminal sliding mode control of dynamic positioning ships with uncertainty and unknown disturbances," *Ocean Engineering*, vol. 281, p. 114925, 2023.
- [14] S. Rozhkov, L. Voronova, and V. Voronov, "Ship Dynamics in the Dynamic Positioning Problem," in *2024 Systems of Signals Generating and Processing in the Field of on Board Communications*, 2024: IEEE, pp. 1-10.
- [15] X. Qian, H. Shen, Y. Yin, and D. Guo, "Nonlinear Model Predictive Control for a Dynamic Positioning Ship Based on the Laguerre Function," *Journal of Marine Science and Engineering*, vol. 12, no. 2, p. 294, 2024.
- [16] M. Zheng, Y. Su, and G. Chen, "An improved sampled-data control for a nonlinear dynamic positioning ship with Takagi-Sugeno fuzzy model," *Mathematical Biosciences and Engineering*, vol. 21, no. 5, pp. 6019-6041, 2024.
- [17] A. J. Sørensen, "A survey of dynamic positioning control systems," *Annual reviews in control*, vol. 35, no. 1, pp. 123-136, 2011.
- [18] T. I. Fossen, "Marine control systems—guidance, navigation, and control of ships, rigs and underwater vehicles," *Marine Cybernetics, Trondheim, Norway, Org. Number NO 985 195 005 MVA*, www.marinecybernetics.com, ISBN: 82 92356 00 2, 2002.
- [19] T. I. Fossen, "Handbook of marine craft hydrodynamics and motion control," *John Willy & Sons Ltd*, 2011.
- [20] Slotine JJ, Li W. Applied nonlinear control. Englewood Cliffs, NJ: Prentice hall; 1991.
- [21] F. Luo, J. Zhang, P. Lyu, Z. Liu, and W. Tang, "Carrier-Based Aircraft Precision Landing Using Direct Lift Control Based on Incremental Nonlinear Dynamic Inversion," *IEEE Access*, vol. 10, pp. 55709-55725, 2022.
- [22] F. Jiang, F. Pourpanah, and Q. Hao, "Design, Implementation, and Evaluation of a Neural-Network-Based Quadcopter UAV System," *IEEE Transactions on Industrial Electronics*, vol. 67, no. 3, pp. 2076-2085, 2020.
- [23] N. Hovakimyan, F. Nardi, A. J. Calise, and H. Lee, "Adaptive output feedback control of a class of nonlinear systems using neural networks," *International Journal of Control*, vol. 74, no. 12, pp. 1161-1169, 2001.
- [24] Y. Wei, H. Xu, and Y. Xue, "Adaptive Neural Networks-Based Dynamic Inversion Applied to Reconfigurable Flight Control and Envelope Protection Under Icing Conditions," *IEEE Access*, vol. 8, pp. 11577-11594, 2020.
- [25] Y. Zhang, J. Gao, Y. Chen, C. Bian, F. Zhang, and Q. Liang, "Adaptive neural network control for visual docking of an autonomous underwater vehicle using command filtered backstepping," *International Journal of Robust and Nonlinear Control*, vol. 32, no. 8, pp. 4716-4738, 2022.
- [26] W. Gai, H. Wang, J. Zhang, and Y. Li, "Adaptive neural network dynamic inversion with prescribed performance for aircraft flight control," *Journal of applied mathematics*, vol. 2013, no. 1, p. 452653, 2013.
- [27] R. Rysdyk and A. J. Calise, "Robust nonlinear adaptive flight control for consistent handling qualities," *IEEE Transactions on Control Systems Technology*, vol. 13, no. 6, pp. 896-910, 2005.
- [28] C. Li, G. Wang, Y. Fan, and Y. Li, "Adaptive RBF neural network controller design for SRM drives," in *2016 35th Chinese Control Conference (CCC)*, 27-29 2016, pp. 6092-6097 .
- [29] L. Qing and L. Juanxia, "Model and Adaptive Control of Rotor/Wing Compound UAV Based on Derivative-Free Adaptive NDI," in *2021 IEEE 4th International Conference on Electronics Technology (ICET)*, 7-10 ,2021, pp. 960-965 .
- [30] R. Rysdyk and A. Calise, "Fault tolerant flight control via adaptive neural network augmentation," in *Guidance, navigation, and control conference and exhibit*, 1998, p. 4483.
- [31] C. Liu, T. Sun, and Q. Hu, "Synchronization Control of Dynamic Positioning Ships Using Model Predictive Control," *Journal of Marine Science and Engineering*, vol. 9, no. 11, p. 1239, 2021.

[32] L. Xu and Z. q. Liu, "Design of fuzzy PID controller for ship dynamic positioning," in *2016 Chinese Control and Decision Conference (CCDC)*, 28-30 May 2016 2016, pp. 3130-3135.

[33] S. Xu, X. Wang, J. Yang, and L. Wang, "A fuzzy rule-based PID controller for dynamic positioning of vessels in variable environmental disturbances," *Journal of Marine Science and Technology*, vol. 25, no. 3, pp. 914-924, 2020.

[34] J. G. Ziegler and N. B. Nichols, "Optimum settings for automatic controllers," *Transactions of the American society of mechanical engineers*, vol. 64, no. 8, pp. 759-765, 1942.

[35] H. Bao-Gang, G. K. I. Mann, and R. G. Gosine, "A systematic study of fuzzy PID controllers-function-based evaluation approach," *IEEE Transactions on Fuzzy Systems*, vol. 9, no. 5, pp. 699-712, 2001.

[36] X. T. Chen and W. W. Tan, "A type-2 fuzzy logic controller for dynamic positioning systems," in *IEEE ICCA 2010*, 9-11 ,2010, pp. 1013-1018.

[37] W.-J. Chang, G.-J. Chen, and Y.-L. Yeh, "Fuzzy control of dynamic positioning systems for ships," *Journal of Marine Science and Technology*, vol. 10, no. 1, p. 7, 2002.

[38] C. Zhang, L. Wan, and Y. Liu, "Ship Heading Control Based on Fuzzy PID Control," in *2019 34rd Youth Academic Annual Conference of Chinese Association of Automation (YAC)*, 6-8 ,2019, pp. 607-612.

[39] Y. Vaghei and A. Farshidianfar, "Trajectory tracking of under-actuated nonlinear dynamic robots: Adaptive fuzzy hierarchical terminal sliding-mode control," *Journal of AI and Data Mining*, vol. 4, no. 1, pp. 93-102, 2016.

کنترل ردیابی موقعیت ASV مبتنی بر روش دینامیک معکوس به همراه روش های هوشمند

حیدر طوسیان شانديزو^{*}، محسن عرفانی حاجی پور و امیر علی باقری

گروه مهندسی برق گرایش کنترل، دانشگاه فردوسی مشهد، مشهد، ایران.

ارسال ۲۰۲۴/۰۱/۲۱ بازنگری ۲۰۲۴/۰۶/۱۹؛ پذیرش ۲۰۲۴/۰۸/۲۲

چکیده:

این مقاله به بررسی توسعه یک کنترل کننده کارآمد برای دنبال کردن دقیق وسایل نقلیه خودکار سطحی با استفاده از تکنیک کنترل دینامیک معکوس می پردازد. ASV ها با چالش هایی مانند اختلالات محیطی از جمله موج ها و بادهای روبه رو هستند که برای صناعی مانند حمل و نقل دریایی و عملیات نظامی با دقت بالا در ناوبری اساسی هستند. این مقاله رویکردی را پیشنهاد می دهد که کنترل کلاسیک را با روش های هوشمند به منظور کاهش اختلالات و اصلاح خطاهای مدل سازی ادغام می کند. دو روش مبتنی بر کنترل کننده دینامیک معکوس معرفی شده اند: یکی از آن ها از شبکه عصبی پرسپترون با یک عبارت تطبیقی استفاده می کند تا خطاهای مدل سازی در کنترل کننده دینامیک معکوس را جبران کند و دیگری از منطق فازی برای تنظیم پارامترهای کنترل جهت کاهش خطاهای مدل سازی استفاده می کند. هدف از این روش ها بهبود انعطاف پذیری سیستم و دقت ردیابی مسیر است. معیارهای ارزیابی شامل تحلیل پاسخ پله و قابلیت دنبال کردن مسیرهای پیچیده هستند که نتایج مقایسه ای با روش کنترل معمولی PID نشان دهنده نتایج مطلوبی است.

کلمات کلیدی: کلمات کنترل دینامیک معکوس، روش های فازی، شبکه عصبی پرسپترون، دینامیک کشتی، ردیابی موقعیت.